Explosives

International Edition: DOI: 10.1002/anie.201607130
German Edition: DOI: 10.1002/ange.201607130

Hydrogen Peroxide Solvates of 2,4,6,8,10,12-Hexanitro-2,4,6,8,10,12-hexaazaisowurtzitane

*Jonathan C. Bennion, Nilanjana Chowdhury, Jeff W. Kampf, and Adam J. Matzger**

Abstract: *Two polymorphic hydrogen peroxide solvates of 2,4,6,8,10,12-hexanitro-2,4,6,8,10,12-hexaazaisowurtzitane (CL-20; wurtzitane is an alternative name to iceane) were obtained using hydrated α-CL-20 as a guide. These novel H_2O_2 solvates have high crystallographic densities (1.96 and 2.03 g cm^{-3}, respectively), high predicted detonation velocities/pressures (with one solvate performing better than ε-CL-20), and a sensitivity similar to that of ε-CL-20. The use of hydrated materials as a guide will be important in the development of other energetic materials with hydrogen peroxide. These solvates represent an area of energetic materials that has yet to be explored.*

The formation of hydrated materials is a common phenomenon throughout crystal engineering; in the field of pharmaceuticals it is estimated that at least one third of all pharmaceuticals are capable of forming hydrates.[1] In energetic materials, the formation of various (hemi-, mono-, di-, etc.) hydrated materials is also an often encountered problem.[2] For example, the widely used energetic materials octahydro-1,3,5,7-tetranitro-1,3,5,7-tetrazocine (HMX) and 2,4,6,8,10,12-hexanitro-2,4,6,8,10,12-hexaazaisowurtzitane (CL-20) both form $^1/_4$ hydrates, γ-HMX and α-CL-20, respectively, which have inferior detonation properties compared to the respective high-density forms, β-HMX and ε-CL-20. The detonation properties (velocity and pressure) are dependent on the density of a material (higher density translates into higher detonation velocity/pressure). While a hydrate may have a high density, hydration ultimately reduces the effective density of the energetic component(s) and as a result diminishes the performance of the material. Such an erosion of properties is similar to that observed in the case of cocrystals of energetic materials with nonenergetic coformers.[3] This has been overcome through the use of other energetic molecules as coformers. Herein we adapt this concept by using hydrogen peroxide as an energetic replacement for water of hydration in CL-20, thus improving the oxygen balance of the material.

Oxygen balance (OB) is the weight percentage of oxygen released as a result of the complete conversion into neutral molecular components (CO_2, H_2O, N_2, etc.) upon detonation.[4] A positive OB denotes that there is excess oxygen in the system after full conversion, whereas a negative OB refers to an insufficient amount of oxygen and typically results in the generation of carbon soot and lower-oxidized, toxic gases (CO, NO). The more negative the OB, the less gas is generated from the detonation and as a result, the brisance or shattering effect of the material is diminished.[5] The vast majority of traditional energetic materials have a negative OB with respect to CO_2: CL-20 (−11%), HMX (−22%), and 2,4,6-trinitrotoluene [TNT] (−74%). The inclusion of water molecules into the lattice of an energetic material does not lead to an increased OB because the oxygen atoms are already bonded to two hydrogen atoms. However, the ability to incorporate water into the lattice suggested to us that a chemically similar, but more oxidizing solvent could improve rather than degrade the performance. Hydrogen peroxide has seen extensive use as a propellant in both mono- and bi-propellant rockets.[6] H_2O_2 has very low toxicity, minimal environmental impact compared to traditional perchlorate oxidizers, and is also impact/shock-insensitive in concentrated form.

In addition to the use of H_2O_2 in rocket fuels, the peroxy group has seen some application for various energetic materials, such as triacetone triperoxide (TATP), diacetone diperoxide (DADP), hexamethylene triperoxide diamine (HMTD), and more recently for energetic materials containing peroxy acid and hydroperoxy groups.[7] The problem often encountered with these materials is that many of them are very sensitive to both thermal and impact initiation, while also having very poor OBs due to the large amount of carbon contained within the backbones. Meanwhile, DADP was shown to form a series of 1:1 cocrystals with 1,3,5-trihalo-2,4,6-trinitrobenzenes (TXTNB, X = Cl, Br or I) through interaction between the TXTNB coformer and the peroxy moiety.[8] These materials show feasibility for the formation of noncovalent interactions with the peroxy moiety. The substitution of H_2O_2 for water of hydration might be predicted to result not only in noncovalent interactions between the peroxy moieties, but also to allow maintenance of the hydrogen bonding pattern.

The hydrated form of CL-20, α-CL-20, is generally regarded as a $^1/_4$ hydrate, but can also exist as a $^1/_2$ hydrate.[2d] The unit cell of the $^1/_4$ hydrate contains a total of eight CL-20 molecules with sufficient void space to encompass two solvent molecules. The packing coefficient (C_k), a measure of the efficiency with which molecules occupy the unit-cell volume, can be determined by dividing the total molecular volume in a unit cell by the unit-cell volume. By comparing the C_k values of the high-density ε-CL-20 (80.6%) and the lower-density α-CL-20 (77.9%), it is evident that α-CL-20 shows void space

[*] J. C. Bennion, Dr. N. Chowdhury, Dr. J. W. Kampf, Prof. A. J. Matzger
Department of Chemistry and the Macromolecular and Engineering Programm, University of Michigan
930 North University Avenue, Ann Arbor, MI 48109-1055 (USA)
E-mail: matzger@umich.edu
Supporting information and the ORCID identification number(s) for the author(s) of this article can be found under: http://dx.doi.org/10.1002/anie.201607130.

that might be used to include additional solvent molecules. Recently, it has been shown that water can be removed under heating/vacuum from α-CL-20 with little deformation of the lattice parameters.[9] This suggests that the void space could be used for the formation of CL-20 solvates that will remain isostructural to the hydrated α-CL-20.

We present herein two novel polymorphic solvates of CL-20 with H_2O_2, orthorhombic **1** and monoclinic **2**; both materials form in a 2:1 molar ratio of CL-20 and H_2O_2 (Figure 1 shows the structures of the pure components). These materials represent the first examples of solvates with H_2O_2 for any energetic material and may be influential for the further development of novel energetic materials.

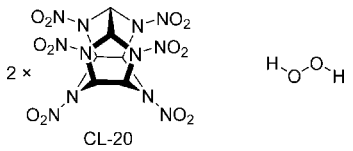

Figure 1. Chemical structures of the pure components for the CL-20 polymorphic solvates **1** and **2**: CL-20 and H_2O_2.

The concomitant formation of **1** and **2** was initially observed from a 1:1 acetonitrile/H_2O_2 (>90% H_2O_2) solution. Solvate **1** exhibits a rhombic habit, whereas **2** typically exhibits a polyhedron habit (see Figures 3c and 4c, respectively), and these crystals were separated and analyzed by powder X-ray diffraction (PXRD). The powder pattern of **1** was indistinguishable from that of α-CL-20 (see Sections 1 and 2 of the Supporting Information), which suggests that the material is either simply α-CL-20 or an isostructural material with H_2O_2 replacing the water molecules as hypothesized. Solvate **2**, on the other hand, is readily distinguishable from any of the other forms of CL-20 (Section 3 of the Supporting Information).

The crystal structures of **1** and **2** were elucidated[15] and determined to be 2:1 CL-20/H_2O_2 solvates (crystallographic data for α-CL-20, **1**, and **2** are presented in Table S1). Both materials have high crystallographic densities at 295 K: 2.033 (**1**) and 1.966 g cm^{-3} (**2**). When compared to α-CL-20 (1.970 g cm^{-3} at 295 K), the isostructural material **1** has a higher density and the density of **2** is similar to that of the hydrated material. The OB for both **1** and **2** was determined to be −8.79%, an improvement with respect to both α-CL-20 (−10.84%) and pure CL-20 (−10.95%).

One way of identifying the solvent content in a crystal structure is using a PLATON/SQUEEZE calculation, which assesses the electron density contribution in the unit cell caused by the solvent.[10] Both the H_2O_2 solvent present in the crystal structure of **1** and the H_2O in α-CL-20 (for these calculations the crystal structure of α-CL-20 was redetermined) sit on the same inversion center, leading to uncertainty regarding the existence of H_2O_2 in the material. The electron density was estimated to be 24 and 44 e$^-$ per unit cell for α-CL-20 and **1**, respectively. The electron density for α-CL-20 corresponds roughly to the two water molecules present in the unit cell (10 e$^-$ per molecule), whereas the higher electron density of 44 electrons for **1** corresponds to the presence of H_2O_2 (18 e$^-$ per molecule) in this material. The same routine was applied to **2**, and the electron density was determined to be 79 e$^-$ per unit cell, which corresponds closely to the four H_2O_2 molecules in the 2:1 CL-20 solvate. The higher electron density suggests the presence of a novel material compared to α-CL-20, but given the tendency of SQUEEZE to overcount electron density, additional investigation using Raman spectroscopy and chemical analysis was carried out to further support this result.

The Raman spectra of both **1** and **2** were compared to all known forms of CL-20 and in particular to α-CL-20 (Figure 2

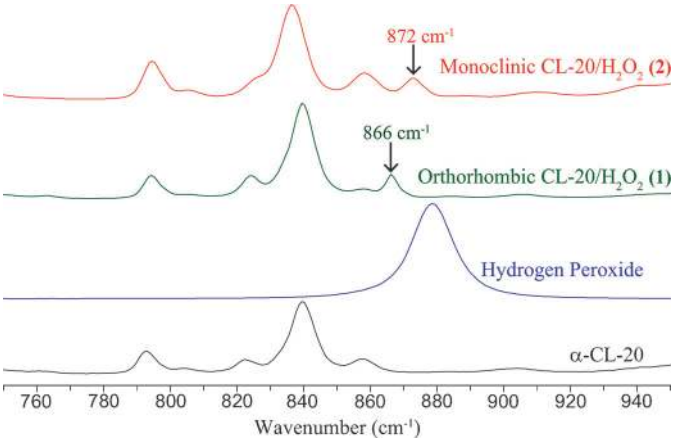

Figure 2. Raman spectra (700–1000 cm^{-1}) of α-CL-20, concentrated H_2O_2, **1**, and **2**. The O–O peak of pure H_2O_2 is at 879 cm^{-1}.

and Section 4 of the Supporting Information). The spectra of both **1** and **2** resemble that of α-CL-20, with the exception of the addition/shifting of the O–O stretching present in the two new solvates. The O–O stretching frequency of pure H_2O_2 is at around 879 cm^{-1}, while the solvates have an O–O peak shifted to 866 and 872 cm^{-1}, respectively, for **1** and **2** (Figure 2). Additionally, shifting is present in the H–O stretching region for all three materials: α-CL-20 (3610 cm^{-1}), **1** (3557 cm^{-1}), and **2** (3517 cm^{-1}). The addition of the O–O peak and the shifting of the H–O peak in both **1** and **2** are indicative of an interaction between CL-20 and H_2O_2. For both solvates, the higher electron density and the new and shifted peaks in the Raman spectra confirm the presence of H_2O_2. This presence of H_2O_2 was also quantified by a chemical test wherein the oxidation of triphenylphosphine with H_2O_2 to triphenylphosphine oxide was measured by ^{31}P NMR spectroscopy and the proposed stoichiometry of two CL-20 to one H_2O_2 was confirmed.

The formation of both CL-20 solvates relies on hydrogen bonding between H_2O_2 and the nitro groups of CL-20 as well as C–H hydrogen bonds between adjacent CL-20 molecules. The shortest interactions between H_2O_2 and CL-20 are highlighted in Figure 3a and 4a, respectively, for **1** and **2**. The H_2O_2 molecule in **1** hydrogen bonds with two CL-20 molecules and interacts with two nitro groups on each molecule in a bifurcated fashion, with intermolecular distances of 2.17/2.22 Å and 2.19/2.24 Å for each CL-20 molecule (Figure 3a). In contrast, the H_2O_2 molecule in solvate **2**

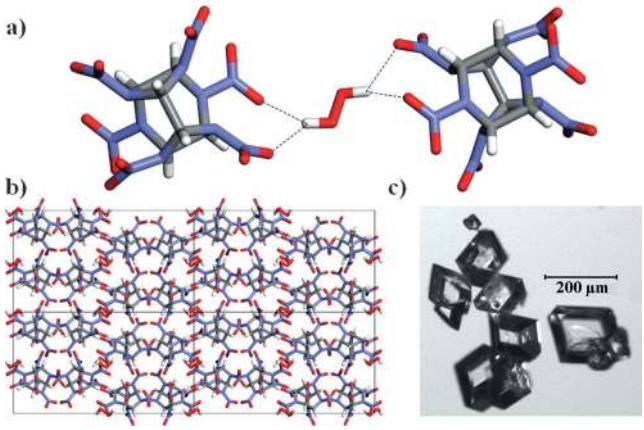

Figure 3. The 2:1 solvate **1**. a) Hydrogen bonding interaction between CL-20 and H_2O_2. b) Unit cell viewed down the *a*-axis. c) Typical rhombic habit morphology of this orthorhombic polymorph.

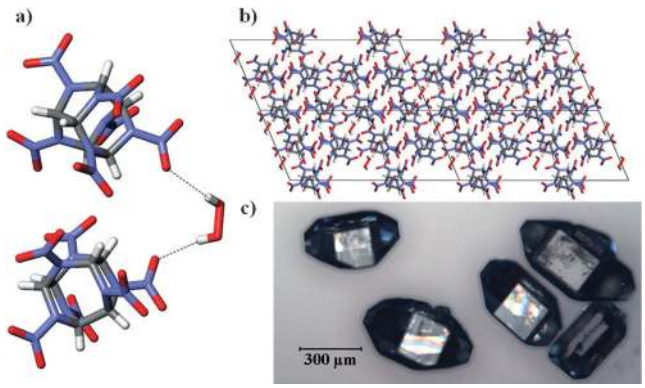

Figure 4. The 2:1 solvate **2**. a) Hydrogen bonding interaction between CL-20 and H_2O_2. b) Unit cell viewed down the *a*-axis. c) Typical polyhedron habit morphology of this monoclinic polymorph.

hydrogen bonds with two CL-20 molecules, with an equivalent intermolecular distance of 2.25 Å. In both structures, the CL-20 molecules form linear chains through hydrogen bonding between C–H and nitro groups of adjacent CL-20 molecules; these interactions are reminiscent of those seen in both 1:1 CL-20/TNT and 2:1 CL-20/HMX.[11] The shortest hydrogen bonds between C–H and NO_2 groups of CL-20 for **1** and **2** are 2.20 Å and 2.23/2.31 Å, respectively. The same linear chain of CL-20 molecules as in **1** is also seen in α-CL-20 (2.28 Å). Additionally in the structure of **2**, the repeat unit of two CL-20 molecules with one H_2O_2 molecule (Figure 4a) forms a tape that extends through C–H hydrogen bonding between adjacent CL-20 molecules at 2.23 Å.

With the structural parameters obtained, the C_k values for **1**, **2**, and the pure components ε-CL-20 and α-CL-20 were determined.[12] The C_k values of both solvates **1** (80.6%) and **2** (78.1%) are higher than the value for α-CL-20 (77.9%), whereas the C_k values of **1** and ε-CL-20 are identical (80.6%). The C_k difference between **1** and α-CL-20 is expected for two reasons: the higher content of solvate molecules for CL-20/H_2O_2 (2:1) compared to CL-20/H_2O (4:1) and the bigger size/volume of H_2O_2 compared to H_2O. The C_k value of solvate **1** equals that of ε-CL-20 through the incorporation of additional oxidizer, while also having a density on par to that of ε-CL-20 (2.04 $g\,cm^{-3}$).

The thermal properties of both **1** and **2** were determined using differential scanning calorimetry (DSC) and thermogravimetric analysis (TGA). The DSC traces show endothermic peaks at 165, 190, and 158 °C for **1**, **2**, and α-CL-20, respectively, and decomposition around 250 °C for all three materials (Section 9 in the Supporting Information). Raman spectroscopy and PXRD were performed after holding the temperature just past the respective endothermic peaks of **1** and **2**, and this thermal event was determined to correspond to the release of H_2O_2 and subsequent conversion to γ-CL-20. The difference in the desolvation temperature of the two materials arises from the difference in both the hydrogen bonding between the two components and the packing arrangement of the CL-20 molecules in the unit cell; in **1** there is a channel for H_2O_2 to escape from, while the H_2O_2 molecule in **2** is contained in a cage of CL-20 molecules. The conversion of the solvates into γ-CL-20 explains why all three materials decompose at the same temperature. Furthermore, the TGA thermograms show the loss of H_2O_2 at the corresponding endothermic-peak temperatures (Sections 10 and 11 of the Supporting Information). The thermal stability of these materials is an important performance criterion to consider in their future application as energetic materials.

The sensitivity of an energetic material to various external stimuli (impact, friction, electrostatic shock, etc.) must be determined before the utility of a material can be fully realized. The sensitivity of **1** and **2** was determined by small-scale impact drop testing; for reference, the 50% impact height (H_{50}) of ε-CL-20 and β-HMX is 29 and 55 cm, respectively (see the Supporting Information).[11b,13] Solvate formation of CL-20 with H_2O_2 results in material **1** having a sensitivity (24 cm) just below that of ε-CL-20 (29 cm). The sensitivity of solvate **2** (28 cm) is similar to that of ε-CL-20, yet with an increase in the overall OB of the system. These materials can be classified as sensitive secondary explosives. Currently CL-20 has seen some application in propellants, but with the need of oxidizers in the final formulation. Both **1** and **2** represent materials that, through solvate formation, are able to reduce/eliminate the need for the use of toxic oxidizers like perchlorates in the formulation of CL-20 propellants and should increase their potential utility.

The detonation properties (velocity, pressure, etc.) were calculated using the thermochemical code Cheetah 7.0.[14] Cheetah calculations require both the chemical (molecular formula, density) and the thermodynamic (heat of formation) properties of a novel energetic material or formulation to predict the detonation velocity/pressure. The cocrystal/solvate performance properties are predicted by treating the materials as a formulation of the two components in their respective molar ratios. For all compounds, the room temperature (295 K) density was used to predict the velocity and pressure of the detonation (Figure 5). Both **1** (9606 $m\,s^{-1}$ and 47.005 GPa) and **2** (9354 $m\,s^{-1}$ and 43.078 GPa) have predicted detonation velocities and pressures that outperform α-CL-20, β-HMX, and the 2:1 CL-20/HMX cocrystal. The orthorhombic solvate **1** is also projected to surpass the properties of ε-CL-20 (9436 $m\,s^{-1}$ and 45.327 GPa), the gold

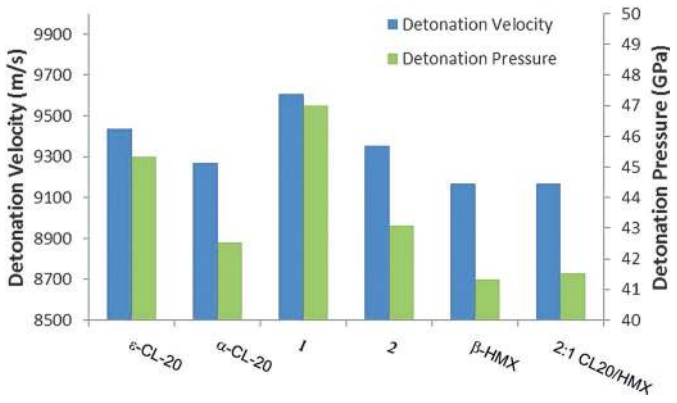

Figure 5. Detonation parameters (velocity and pressure) of ε-CL-20, α-CL-20, **1**, **2**, β-HMX, and 2:1 CL-20/HMX, predicted with Cheetah 7.0 using the room-temperature (295 K) crystallographic density of each material; detonation parameters for **1** at 2.033 g cm^{-3} were calculated by extrapolating the detonation velocity vs. density and detonation pressure vs. density squared from the values determined at 99–90% of the crystallographic density given that the theoretical maximum density maxed out at only 2.013 g cm^{-3}.

standard for high-performance energetic materials; this feat is accomplished through the incorporation of H_2O_2 to increase the overall OB, with little degradation to the sensitivity of the material.

In conclusion, we have discovered and characterized two polymorphic energetic solvates containing highly explosive CL-20 and the oxidizer H_2O_2 in a 2:1 molar ratio. The hydrated form of CL-20, α-CL-20, was used as a guide for the synthesis of the two H_2O_2 solvates, and indeed one solvate remained isostructural to α-CL-20. These solvates represent the first example of hydrogen bonding interactions between H_2O_2 and the nitro moiety, and the approach will be useful for the formation of additional materials containing H_2O_2 solvate. Detonation parameters (velocity and pressure) of the two solvates are predicted to surpass the performance of all known forms of HMX and all low-density forms of CL-20, with the orthorhombic solvate **1** expected to exceed the properties of even ε-CL-20. The incorporation of H_2O_2 into the crystal system allows for an easy and effective method for the improvement of detonation properties, without the need to develop new compounds. By using existing hydrated energetic materials as a guide, the formation of additional isostructural H_2O_2 solvates may be realized, which should perform better than their pure energetic polymorphs.

Acknowledgements

This work was supported by the Army Research Office (ARO) in the form of a Multidisciplinary University Research Initiative (MURI) (grant number: W911NF-13-1-0387). We thank Dr. Antek Wong-Foy for helpful discussions related to the NMR experiments.

Keywords: explosives · hydrates · oxygen balance · sensitivity · solvates

How to cite: *Angew. Chem. Int. Ed.* **2016**, *55*, 13118–13121
Angew. Chem. **2016**, *128*, 13312–13315

[1] H. G. Brittain, *Drugs Pharm. Sci.* **1999**, *95*, 128.
[2] a) E. V. Nikitina, G. L. Starova, O. V. Frank-Kamenetskaya, M. S. Pevzner, *Kristallografiya* **1982**, *27*, 485; b) R. Haiges, G. Belanger-Chabot, S. M. Kaplan, K. O. Christe, *Dalton Trans.* **2015**, *44*, 7586–7594; c) P. Main, R. E. Cobbledick, R. W. H. Small, *Acta Crystallogr. Sect. C* **1985**, *41*, 1351–1354; d) A. T. Nielsen, A. P. Chafin, S. L. Christian, D. W. Moore, M. P. Nadler, R. A. Nissan, D. J. Vanderah, R. D. Gilardi, C. F. George, J. L. Flippen-Anderson, *Tetrahedron* **1998**, *54*, 11793–11812; e) A. A. Dippold, T. M. Klapötke, *Chem. Eur. J.* **2012**, *18*, 16742–16753; f) H. Gao, J. N. M. Shreeve, *Chem. Rev.* **2011**, *111*, 7377–7436.
[3] a) K. B. Landenberger, A. J. Matzger, *Cryst. Growth Des.* **2010**, *10*, 5341–5347; b) K. B. Landenberger, A. J. Matzger, *Cryst. Growth Des.* **2012**, *12*, 3603–3609; c) D. I. A. Millar, H. E. Maynard-Casely, D. R. Allan, A. S. Cumming, A. R. Lennie, A. J. Mackay, I. D. H. Oswald, C. C. Tang, C. R. Pulham, *CrystEngComm* **2012**, *14*, 3742–3749.
[4] The OB for an organic material can be calculated using the following equation: $-1600(2a+0.5b-d)$/MW, where a, b, c, d are the numbers of carbon, hydrogen, nitrogen, and oxygen atoms, respectively, and MW is the molecular weight of the material.
[5] a) W. C. Lothrop, G. R. Handrick, *Chem. Rev.* **1949**, *44*, 419–445; b) A. Mustafa, A. A. Zahran, *J. Chem. Eng. Data* **1963**, *8*, 135–150.
[6] a) S. Bonifacio, G. Festa, A. R. Sorge, *J. Propul. Power* **2013**, *29*, 1130–1137; b) O. V. Romantsova, V. B. Ulybin, *Acta Astronaut.* **2015**, *109*, 231–234; c) J. J. Rusek, *J. Propul. Power* **1996**, *12*, 574–579.
[7] a) N.-D. H. Gamage, B. Stiasny, J. Stierstorfer, P. D. Martin, T. M. Klapötke, C. H. Winter, *Chem. Commun.* **2015**, *51*, 13298–13300; b) N.-D. H. Gamage, B. Stiasny, J. Stierstorfer, P. D. Martin, T. M. Klapötke, C. H. Winter, *Chem. Eur. J.* **2016**, *22*, 2582–2585; c) R. Matyáš, J. Pachman, *Propellants Explos. Pyrotech.* **2010**, *35*, 31–37; d) A. Wierzbicki, E. A. Salter, E. A. Cioffi, E. D. Stevens, *J. Phys. Chem. A* **2001**, *105*, 8763–8768.
[8] a) K. B. Landenberger, O. Bolton, A. J. Matzger, *Angew. Chem. Int. Ed.* **2013**, *52*, 6468–6471; *Angew. Chem.* **2013**, *125*, 6596–6599; b) K. B. Landenberger, O. Bolton, A. J. Matzger, *J. Am. Chem. Soc.* **2015**, *137*, 5074–5079.
[9] L. Pu, J.-J. Xu, X.-F. Liu, J. Sun, *J. Energ. Mater.* **2016**, *34*, 205–215.
[10] A. L. Spek, *Acta Crystallogr. Sect. C* **2015**, *71*, 9–18.
[11] a) O. Bolton, A. J. Matzger, *Angew. Chem. Int. Ed.* **2011**, *50*, 8960–8963; *Angew. Chem.* **2011**, *123*, 9122–9125; b) O. Bolton, L. R. Simke, P. F. Pagoria, A. J. Matzger, *Cryst. Growth Des.* **2012**, *12*, 4311–4314.
[12] Molecular volumes were calculated using Spartan14 V1.1.2 by determining the equilibrium geometry at the ground state for structures of the pure components with the semi-empirical AM1 method.
[13] J. C. Bennion, A. McBain, S. F. Son, A. J. Matzger, *Cryst. Growth Des.* **2015**, *15*, 2545–2549.
[14] Cheetah 7.0 calculations were preformed with the Sandia JCZS product library revision 32.
[15] CCDC 1495519 (**1**), 1495520 (**2**), and 1495521 (α-CL-20) contain the supplementary crystallographic data for this paper. These data are provided free of charge by The Cambridge Crystallographic Data Centre.

Received: July 22, 2016
Published online: September 16, 2016

